

# De novo construction of q-ploid linkage maps using discrete graphical models

P. Behrouzi

Wageningen University and Research Centre  
[pariya.behrouzi@wur.nl](mailto:pariya.behrouzi@wur.nl)

E. C. Wit

University of Groningen  
[e.c.wit@rug.nl](mailto:e.c.wit@rug.nl)

September 3, 2022

## Abstract

Linkage maps are important for fundamental and applied genetic research. New sequencing techniques have been created opportunities to increase substantially the density of genetic markers. With such revolutionary advances in technology come new challenges in methodologies and informatics. In this article, we introduce a novel linkage map algorithm to construct high-quality and high-density linkage maps for diploid and polyploid species. We propose to construct linkage maps using graphical models either via a sparse Gaussian copula or via a nonparanormal skeptic approach. Linkage groups (LGs), typically chromosomes, and the order of markers in each LG is determined by revealing the conditional independence relationships among a large number of markers in the genome. We illustrate the efficiency of the inference method on a broad range of synthetic data with varying rates of missingness and genotyping errors. We show that our method outperforms other available methods in terms of determining the correct number of linkage groups and ordering markers both when the data are clean and contain no missing observations and when data are noisy and incomplete. In addition, we implement the method on real genotype data of barley and potato from diploid and tetraploid populations, respectively. Given that most tetraploid potato linkage maps have been generated either from diploid populations (Felcher et al., 2012) or from a subset of marker types (e.g. both parents were heterozygous) (Grandke et al., 2017), developing a map construction method based on discrete graphical models opens the opportunities to construct high-quality linkage maps for any biparental diploid and polyploid

species containing all different marker types. We have implemented the method in the R package `netwgwas`.

**Keywords:** Graphical models; Latent variable; Gaussian Copula; Linkage mapping; Diploid; Polyploid; High-throughput data.

## 1 Introduction

A linkage map provides a fundamental resource to understand the order of markers for the vast majority of species whose genome are yet to be sequenced. Furthermore, it is an essential ingredient in the often used QTL mapping of genetic diseases. In particular to identify responsible genes for heritable or other types of diseases in humans or to identify traits such as, disease resistance in plants or animals.

The recent advances in sequencing technology make it possible to comprehensively sequence huge numbers of markers, construct dense maps and ultimately create a foundation for studies on genome structure, genome evolution, identification of quantitative trait loci (QTLs) and understanding the inheritance of multi-factorial traits. Next-generation sequencing (NGS) techniques offer massive and cost-effective sequencing throughput. However, they also bring new challenges in constructing high-quality linkage maps. The NGS data can suffer from high rates of genotyping errors which means the observed genotype for an individual is not necessarily identical to its true genotype. Under such circumstances, constructing high-quality linkage map can be difficult. Each species is categorized as diploid or polyploid by comparing their chromosome number.

Diploids have two copies of each chromosome. For diploid species many algorithms for constructing linkage maps have been proposed. Some of them have been implemented into user-friendly softwares, such as R/qtl (Broman et al., 2003), JOINMAP (Jansen et al., 2001), OneMap (Margarido et al., 2007), MSTMAP (Wu et al., 2008). Among the constructing genetic map algorithms, R/qtl estimates genetic maps and identifies genotyping errors in relatively small set of markers. JOINMAP is a commercial software that widely used in the genetic scientific community. It uses two methods to construct genetic maps, one is based on regression (Stam, 1993) and the other uses a Monte Carlo multipoint maximum likelihood (Jansen et al., 2001). OneMap has been reported to construct linkage maps in non-inbred populations. However, it is computationally expensive. The MSTMap is a fast genetic map algorithm that determines the order of markers by computing the minimum spanning tree of an associated graph.

Polyploidy is the condition whereby a biological cell or organism has more than two chromosome sets. Polyploidy is very common in flowering plants and in different crops such as watermelon, potato, bread wheat, etc., which contain three (triploid), four (tetraploid), and six (hexaploid) sets of chromosomes respectively. Despite of

the importance of polyploid species, the research and statistical tools for their linkage map construction is underdeveloped. Grandke et al. (2017) recently have developed a method to construct linkage map in polyploids. Their method is based on calculating recombination frequencies between marker pairs, then using hierarchical clustering and optimal leaf algorithm to detect chromosomes and order markers. However, the method can be computationally expensive even for a small number of markers. Furthermore, some literatures have been focused on constructing genetic linkage map only for tetraploids that are limited to autotetraploid species. Among them, one has been implemented in a software, TetraploidMap, (Preedy and Hackett, 2016) which needs manual interaction and visual inspection, which limits its implementation. We remark that the current approaches to polyploid map construction are mainly based on estimation of recombination frequency and LOD score (logarithm of the odds ratio) (Wang et al., 2016).

Different diploid and polyploid map construction methods have taken substantial steps to build better-quality linkage maps. However, the existing linkage map methods still suffer from low quality genetic mapping performance, in particular when ratios of genotyping errors and missing observations are high.

The main contribution of this paper is to introduce a novel linkage map algorithm for diploid and polyploid species, and to overcome the difficulties that arise routinely in Next-generation sequencing (NGS) data. In the proposed method, we aim to build high-density and high-quality linkage maps using the statistical property called conditional dependence relationships, which reveals the direct relations among the genetic markers. For diploid scenarios, we evaluate the performance of the proposed method and the other methods in several comprehensive simulation studies both when the input data are clean and do not include missing observations and when the input data are very noisy and incomplete. We measure the performance of the methods in grouping and ordering accuracy scores. In addition, we study the performance of our method in constructing linkage map for simulated polyploids, namely tetraploids and hexaploids. Furthermore, we have applied netgwas to construct map in real-world examples, such as barley genotyping data from a diploid population and potato genotyping data from a tetraploid population.

## 2 Genetic background on linkage map

A linkage map is the linear order of genetic markers on a chromosome. It is used to study the association between genes and traits by geneticist. We are concerned with genetic markers in the form of single nucleotide polymorphisms (SNPs). A SNP may exist in the homozygous state if all  $q$  allele copies (e.g. diploids  $q = 2$ ) are identical, and in the heterozygous state otherwise. For the moment, we assume that each allele can take only one of two values,  $A$  or  $a$ . This can be relaxed without requiring any

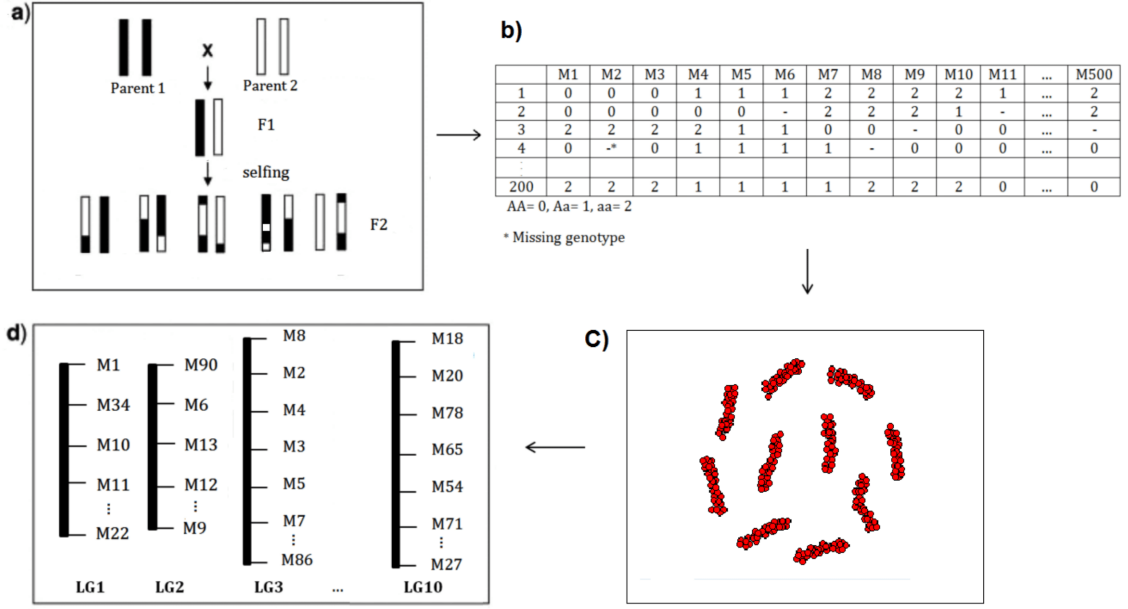


Figure 1: General view of the proposed linkage map estimation process. For the sake of illustration we use diploid population which contain two copies of each chromosome. (a) shows an example of a mating experiment of an inbred F2 population. (b) reports the derived genotype data for 200 individuals which have genotyped for 500 markers. In (c) the undirected graph between all 500 markers is reconstructed. (d) shows 10 linkage groups (chromosomes) which markers are ordered within each linkage group (LG).

methodological adjustments, more will follow in the discussion. Here, we are dealing with genetic markers from high-throughput data such as next-generation sequencing (NGS) and SNP arrays.

## 2.1 Linkage map for diploids and polyploids

Diploid organisms contain two sets of chromosomes, one from each parent, whereas polyploids contain more than two sets of chromosomes. Polyploids with a particular number of chromosome sets reflect their level of ploidy: triploids have three sets, tetraploids have four, pentaploids have five, and so forth. Here, we refer to diploids and polyploids as  $q$ -ploid  $q \geq 2$ , where in diploids  $q = 2$ , triploids  $q = 3$ , tetraploids  $q = 4$ , and so on.

The genotype of any  $q$ -ploid organism can be homozygous or heterozygous at each single locus on the genome. Different genotype forms of the same gene are called alleles. Alleles can lead to different traits. Alleles are commonly represented by

letters, for example for the gene related to the trait allele could be called A and a. In  $q$ -ploid individuals there are  $q$  copies of allele. If all  $q$  allele copies of an organism are identical, the organism is in homozygous state at that locus and at heterozygous state otherwise. For instance, a tetraploid individual is homozygous for two size alleles A and a, if all 4 alleles copies are either *A*, or *a* which correspond with the genotypes *AAAA* and *aaaa*, respectively. If a tetraploid individual is heterozygous the following three genotypes would appear: one copy of the A allele and three copies of a (e.g. *Aaaa*), two copies of A and two copies of a (e.g. *AAaa*), or three copies of A and one copy of a (e.g. *AAAa*). Unlike existing methods, our method does not only work for diploid organism but also for any polyploids. Obviously, also simple haploid organisms such as haploid yeast cells can be analyzed with our method.

## 2.2 Mapping population

If mating perhaps between two parental lines that have recent common biological ancestors, this called inbreeding. If they have no common ancestors up to e.g. 4-6 generations, this called outcrossing. In both cases, the genome of derived progenies are the random mosaics of the genome of the parents. However, as a consequence of inbreeding parental alleles are distinguishable in the genome of the progeny, whereas in outcrossing this does not hold.

Inbreeding progenies derive from two homozygous parents. Some inbreeding designs, such as *Backcrossing* (BC), lead to a homozygous population where the derived genotype data includes only homozygous genotypes of the parents namely AA and aa (conveniently coded as 0 and 1). Whereas, some other inbreeding designs such as *F2* leads to a heterozygous population where the derived genotype data contains also heterozygous genotypes as well as homozygous ones namely AA, Aa, and aa (conveniently coded as 0, 1 and 2, see Figure 1a and Figure 1b for an example for a diploid species). Many other experimental designs also in use. Not all existing methods for linkage mapping support all inbreeding experimental designs. However, our proposed algorithm constructs a linkage map for any type of biparental inbreeding experimental designs. In fact, unlike other existing methods, specifying the population type in our approach is not required since our proposed method is broad and handles any population types that contain at least two distinct genotype states.

Outcrossing or outbred experimental designs, such as full-sib families, derive from two non-homozygous parents. Thus, the genome of the progenies include a mixed set of many different marker types containing fully informative markers and partially informative markers (e.g. missing markers). Markers are called fully informative because all of the resulted gamete types can be phenotypically distinguished on the basis of their genotypes, whereas partially informative markers are the gamete types that have identical phenotypes.

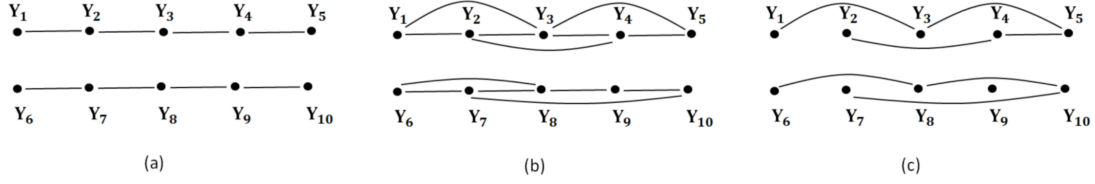


Figure 2: A cartoon example of conditional dependence pattern between neighboring markers in different population types: (a) homozygous (b) inbred, and (c) outcrossing (outbred) populations, where the ordered markers  $Y_1, \dots, Y_5$  reside on chromosome 1 and  $Y_6, \dots, Y_{10}$  on chromosome 2.

### 2.3 Meiosis and Markov dependence

During meiosis, chromosomes pair and exchange genetic material (crossover). In diploids two chromosomes pair at meiosis. In polyploids the  $q$  chromosome copies may happen to form different types of multivalent pairing. For example, in tetraploids may all four chromosome copies pair at meiosis.

Assume a sequence of ordered SNP markers  $X_1^c, X_2^c, \dots, X_d^c$  along chromosome  $c$  in a  $q$ -ploid species. We describe the Markov dependence structure between markers for different populations schemes. (i) During meiosis in inbred populations, genetic material from one of the two parents is copied into the offspring in a sequential fashion, i.e., reading along the genome, until in a random fashion the copying switches to the other parent. Thus, the genome of the offspring is the random mosaics of the genome of its parents. The genotype state at each chromosomal region, locus, of the offspring is either homozygous from maternal, heterozygous, and homozygous from paternal. As a result of genetic linkage and crossover, for instance, a homozygous of maternal genotype will typically be followed by a heterozygous genotype, before being able to be followed by a homozygous paternal genotype.

*Genetic linkage* states that markers located close to one another on a chromosome tend to be inherited together during meiosis. Thus, due to *genetic linkage*, neighboring markers across a chromosome are linked. Another key biological fact during meiosis is that markers that are on different chromosomes segregate independently, which is the *independent assortment law*.

For example, consider scheme (i) consisting of only a homozygous population, the random variable  $Y_j$  which represents genotype of an individual at location  $j$  can be defined as

$$Y_j = \begin{cases} 1 & \text{paternal marker at locus } j \text{ on homologous k,} \\ 0 & \text{otherwise.} \end{cases}$$

This scheme occurs in inbred homozygous populations that include only two genotype states namely homozygous maternal and homozygous paternal. Mapping pop-

ulations, such as backcrossing, are included in this scheme. Let  $y_j$  be two possible genotype states at location  $j$ , then under the assumption of no crossover interference – which states that when a crossover has formed, another crossover is prevented from forming in close proximity – the recombination frequency between the two locations  $j$  and  $j + 1$  is independent of recombination in the other locations on genome. So, the following holds

$$Pr(Y_{j+1} = y_{j+1} \mid Y_j = y_j, Y_{j-1} = y_{j-1}, \dots, Y_1 = y_1) = Pr(Y_{j+1} = y_{j+1} \mid Y_j = y_j) \quad (1)$$

This equation indicates that genotype of a marker at location  $j + 1$  is conditionally independent of genotypes at locations  $j - 1, j - 2, \dots, 1$  given a genotype at location  $j$ . This can be written as

$$Y_{j+1} \perp\!\!\!\perp (Y_1, \dots, Y_{j-1}) \mid Y_j \quad (2)$$

This defines a discrete graphical model  $G = (V, E)$  which consist of vertices  $V = \{1, \dots, p\}$  and edge set  $E \subseteq V \times V$  with a binary random variable  $Y_j \in \{0, 1\}^p$ . Given the above property between neighboring markers, we construct linkage maps using conditional (in)dependence models. Figure 2a shows a cartoon image of conditional (in)dependencies for this scheme.

Scheme (ii): In inbred populations, one complication arises when in the genotype data we cannot identify each homologue due to heterozygous genotypes.  $Q$ -ploid ( $q \geq 2$ ) heterozygous inbred populations, like  $F2$ , are examples of such cases, where we define  $X_{jk}$  as

$$X_{jk} = \begin{cases} 1 & \text{if marker } j \text{ on homologous } k \text{ is of type } A, \\ 0 & \text{otherwise} \end{cases}$$

where  $A$  is one of the two possible alleles at that specific location. Here,  $X_{jk}$  represents allele at homologous  $k$  of a chromosome where the genotype in that location can be written as  $X_j = \{X_{j1} \dots X_{jq}\}$ . For example at marker location  $j$ ,  $X_j = Aaaa$  is one possible genotype for a tetraploid species ( $q = 4$ ); it includes one copy of the desirable allele  $A$  where  $X_{j1} = A$ ,  $X_{j2} = a$ ,  $X_{j3} = a$ , and  $X_{j4} = a$  represent the alleles in the first, second, third and fourth homologous, respectively. The other possible genotypes which include one copy of the desired allele are  $aAaa$ ,  $aaAa$ ,  $aaaA$ . It is typically impossible to distinguish between genotypes with the same number of copies of a desired allele (e.g.  $Aaaa$ ,  $aAaa$ ,  $aaAa$ ,  $aaaA$ ), therefore we take a random varibale  $Y_j$  as observed the number of  $A$  alleles at location  $j$ :

$$Y_j = \sum_{k=1}^q X_{jk}. \quad (3)$$

Table 1 shows an example of correspondence between  $Y_j$  and  $X_j$  for a  $q$ -ploid species when  $q = 4$ . We remark that a  $q$ -ploid species contains  $q + 1$  genotype states at location  $j$ , as it has shown in Table 1 for a tetraploid species.

Due to the *genetic linkage*, the sequence of ordered SNP markers  $Y_1, Y_2, \dots, Y_d$  forms a Markov chain as equation (1) with the state space  $S$  which contains  $q + 1$  states. Therefore, the conditional (in)dependence relationships (2) between neighboring markers is held. Figure 2b represent the cartoon image of conditional independence graph for this scheme.

Table 1

The number of copies (dosage) of a reference allele. The relation between different genotypes,  $X_{j.}$ , and the allele dosage,  $Y_j$ , for a tetraploid individual, where  $A$  is the reference allele.

$Y_j$	$X_{j.}$
0	<i>aaaa</i>
1	<i>Aaaa, aAaa, aaAa, aaaA</i>
2	<i>AAaa, AaAa, AaAa, AaaA, aaAA</i>
3	<i>AAAa, AaAA, AAaA, AAAa, aAAA</i>
4	<i>AAAA</i>

Scheme (iii): In outcrossing (outbred) populations, unlike inbred populations, we do not know – or it is not well defined – what “parental” means. In other words, markers in the genome of the progenies can not be easily assigned to their parental homologous. For example, if both non-homozygous parents contain  $A_j A_j A_j A_j$  genotype at marker location  $j$ , then offspring will also have  $A_j A_j A_j A_j$  genotype at marker location  $j$ . But, we do not know whether that genotype belongs to paternal or maternal homologous, since both parents have  $A_j A_j A_j A_j$  genotype at marker location  $j$ . So, in this case we define  $X_{jk}$  as follow

$$X_{jk} = \begin{cases} 1 & \text{if marker } j \text{ on homologue } k \text{ is of type } A_j, \\ 0 & \text{otherwise} \end{cases}$$

where  $A_j$  is one of the possible parental alleles at location  $j$ . So, random variable  $Y_j$  which presents the dosage of alleles can be defined as equation (3). Furthermore, in polyploids the *linkage* depends on how a single chromosome pair during meiosis to generate gametes. In this regard, if both polyploid parents have  $A_j$  allele in all  $q$  haploid, then offspring will also have it and this will not co-vary with neighboring markers. The possibility of different pairing models during meiosis makes the situation more complex. In diploids, the two homologous chromosomes pair up and form a bivalent then cross-over before recombinations occur. But polyploids meiosis can occur in various ways, in tetraploids four homologous chromosomes can form either two separate bivalent during meiosis, each of which contributes one haploid like diploids, or alternatively, in a more complex situation, the four homologous chromosomes can

form quadrivalent, such that cross-over occurs between eight haploids. In both pairing models, bivalent or quadrivalent, crossover events result in recombined haploids that are mosaics of parental chromosomes. Outbred progenies are genetically diverse and highly heterozygous, whereas inbred individuals have little or no genetic variation due to inbreeding.

The term (1) partially holds for the scheme (iii) where a discrete graphical model can be defined for a multinomial variables  $Y_j = \{0, 1, \dots, q\}$ . We use conditional independences to construct linkage maps in outbred populations. However, in this type populations due to a mixed set of different marker types the conditional independence relationship between neighboring markers may be more complicated. Many genetic assumptions made in traditional linkage analyses (e.g., known parental linkage phases throughout the genome) do not hold here. For example in a case that parents have both  $A_j$  allele, then offspring will also have it but this will not covary with neighboring markers. Figure 2c shows a cartoon example of such graphs.

To summarize, term (1) holds for schemes (i) and (ii), and partially (iii) because transition probability from a genotype at location  $j$  to a genotype at location  $j + 1$  depends on the recombination frequency between the two locations  $j$  and  $j + 1$ , which is independent of recombination in the other locations. This presents a discrete markov process  $\{Y_j\}_{j=1, \dots, d}$  with a state space  $S$  which contains  $q + 1$  genotype states and a transition matrix which in case of polyploids ( $q \geq 3$ ), it can be calculated regarding the mode of chromosomal pairing (e.g. bivalent or quadrivalent). The Markov structure of the SNP markers in the all three schemes yields a graphical model with as many node as markers in a genome. The random variable  $Y_j$  follows a discrete graphical model that the joint distribution  $P(Y)$  can be factorized as,

$$P(Y) = \prod_{c=1}^C \prod_{j=1}^p f_{j,j+1}^{(c)}(Y_j^{(c)}, Y_{j+1}^{(c)}), \quad (4)$$

where  $C$  defines the number of chromosomes in a genome, and  $p_c$  stands for the number of markers in chromosome  $c$ . The outer multiplication of (4) shows the *independent assortment law*, and the inner multiplication represents the *genetic linkage* between markers within a chromosome where the factor  $f_{j,j+1}^{(c)}$  defines the conditional dependence between adjacent markers given the rest of the markers. Through this probabilistic insight, the inferred conditional (in)dependence relationships between markers provides a skeleton for the construction of linkage map.

### 3 Algorithm to detect linkage map

We propose to build a linkage map in two steps. First, reconstructing an undirected graph for all SNP markers on a genome. Second, determining the correct order

of markers in the obtained linkage groups from the first step. We also show how our method handles genotyping errors and missing observations in reconstructing a linkage map.

### 3.1 Estimating marker-marker network

To reconstruct an undirected graph between SNP markers in a  $q$ -ploid species we propose two methods, sparse ordinal glasso (Behrouzi & Wit, 2017a) and the nonparamormal skeptic approach (Liu et al., 2012) (discussed in the supplementary materials). The former method can deal with missing values, whereas the latter is computationally faster.

An undirected graphical model for the joint distribution (4) of a random vector  $Y = (Y_1, \dots, Y_p)$  is associated with a graph  $G = (V, E)$ , where each vertex  $j$  corresponds to a variable  $Y_j$ . The pair  $(j, l)$  is not an element of the edge set  $E$  if and only if  $Y_j$  is independent of  $Y_l$  given the rest of the variables. In the graph estimation problem, we have  $n$  observations of the random vector  $Y$ , and it is our aim to estimate the edge set  $E$ . Depending on how various mapping populations are produced,  $Y$  represents either binary variables  $Y = \{0, 1\}$ , like in homozygous populations, or multinomial variables  $Y = \{0, 1, \dots, q + 1\}$  where  $q$  is the ploidy level. For example in diploids  $q$  is 2 and in tetraploids 4.

**Sparse ordinal glasso** A relatively straightforward approach to discover the conditional (in)dependence relation among markers is to assume underlying continuous variables  $Z_1, \dots, Z_p$  for markers  $Y_1, \dots, Y_p$  which can not be observed directly. In our modeling framework, we remark that  $Y_j$  and  $Z_j$  define observed rank and true latent value respectively, where each latent variables in one-to-one correspondence with the observed variables. The relationship between  $Y_j$  and  $Z_j$  is expressed by a set of cut-points  $(-\infty, C_1^{(j)}], (C_1^{(j)}, C_2^{(j)}], \dots, (C_q^{(j)}, \infty)$  which is obtained by partitioning the range of  $Z_j$  into  $q_j - 1$  disjoint intervals. Thus,  $y_j^{(i)}$ , which represents the genotype of the  $n$ -th individual for the  $j$ -th marker, can be written as follows

$$y_j^{(i)} = \sum_{k=1}^q k \times 1_{\{c_{q-1}^{(j)} < z_j^{(i)} \leq c_q^{(j)}\}} \quad i = 1, 2, \dots, n. \quad (5)$$

We use a high dimensional Gaussian copula with discrete marginals. We assume

$$Z \sim N_p(0, \Sigma)$$

where the  $p \times p$  precision matrix  $\Theta = \Sigma^{-1}$  contains all the conditional independence relationship between variables. Given our interest parameter  $\Theta$  we nonparametrically

estimate the cut-points for each  $j = 1, \dots, p$  as follows

$$\widehat{C}_q^{(j)} = \begin{cases} -\infty & \text{if } q = 0; \\ \Phi^{-1}(\sum_{i=1}^n I(y_j^{(i)} \leq q)/n) & \text{if } q = 1, \dots, q_j - 1; \\ +\infty & \text{if } q = q_j. \end{cases}$$

**Penalized EM algorithm** In genotype datasets we commonly encounter situations that the number of genetic markers  $p$  exceeds the number of individuals  $n$ . To solve this dimensionality problem we propose to impose an  $l_1$  norm penalty on the likelihood consisting of the absolute value of the elements of the precision matrix  $\Theta$ . Furthermore, to be able to deal with commonly occurring missing values in genotype data we implement an EM algorithm (McLachlan and Krishnan, 2007) which iteratively finds the penalized maximum likelihood estimate  $\widehat{\Theta}_\lambda$ . This algorithm proceeds by iteratively computing the conditional expectation of complete log-likelihood and optimizing it for estimating  $\widehat{\Theta}_\lambda$ . Using the extended rank likelihood (Hoff, 2007) in the E-step we compute the expected complete penalized log-likelihood as follow

$$Q_\lambda(\widehat{\Theta} \mid \Theta^{(m)}) = \frac{n}{2} \left[ \log |\Theta| - \text{tr}(\bar{R}\Theta) - p \log(2\pi) \right] - \lambda \|\Theta\|_1 \quad (6)$$

where  $\bar{R} = \frac{1}{n} \sum_{i=1}^n E_{Z^{(i)}}(Z^{(i)} Z^{(i)t} | Y^{(i)}, \widehat{\Theta}^{(m)})$  and  $\lambda$  is a nonnegative tuning parameter. To calculate  $\bar{R}$  we propose two different approaches, namely Gibbs sampling and an approximation method (more details are provided in the supplementary materials). The M-step is a maximization problem which can be solved efficiently using either graphical lasso (Friedman et al., 2008)

$$\widehat{\Theta}_{\text{glasso}}^{(m+1)} = \arg \max_{\Theta} \left\{ \log |\Theta| - \text{tr}(\bar{R}\Theta) - \lambda \|\Theta\|_1 \right\}$$

or the CLIME estimator (Cai et al., 2011)

$$\widehat{\Theta}_{\text{CLIME}}^{(m+1)} = \arg \min_{\Theta} \|\Theta\|_1 \quad \text{subject to} \quad \|\bar{R}\Theta - I_p\|_\infty \leq \lambda,$$

where  $\lambda$  is a tuning parameter and  $I_p$  is a  $p$ -dimensional identity matrix.

In large-scale genotyping studies, it is common to have missing genotype data. We handle the missing data, before determining number of linkage groups and ordering markers, within the E-step of the EM algorithm, where we calculate the conditional expectation of true latent variables given the observed ranks. If an observed value,  $y_j^{(i)}$  is missing, we take the unconditional expectation the corresponding latent variable. In the EM framework we can easily handle high ratios of missingness in the data.

## 3.2 Determining linkage groups

A group of loci that are correlated defines a linkage group (LG). Depending on the density and proximity of the underlying markers each LG corresponds to a chromosome or part of a chromosome. The number of founded linkage groups is controlled by the tuning parameter  $\lambda$  in section 3.1. We use the extended Bayesian criteria (eBIC), which has successfully been applied in selecting sparse Gaussian graphical models for genomic data in Yin and Li (2011), to determine the number of linkage groups. The eBIC is defined as

$$eBIC(\lambda) = -2\ell(\widehat{\Theta}_\lambda) + (\log n + 4\gamma \log p)df(\lambda), \quad (7)$$

where  $\ell(\widehat{\Theta}_\lambda)$  is the non-penalized likelihood,  $df(\lambda) = \sum_{1 \leq d \leq l \leq p} I(\widehat{\Theta}_{\lambda} \neq 0)$ , and  $\gamma \in [0, 1]$  is an additional parameter. In case of  $\gamma = 0$  the classical BIC is obtained. Typical values for  $\gamma$  are  $1/2$  and  $1$ . We select the value of  $\lambda$  that minimizes (7) for  $\gamma = \frac{1}{2}$ .

It is notable that in existing map construction methods the construction of linkage groups is usually done by manually specifying a threshold for pairwise recombination frequencies which influence the output map, whereas our method detects LGs automatically.

Two biological concepts, called the *independent assortment law* and *genetic linkage*, are crucial in understanding the concept of linkage groups in graphical model framework. The former states that markers at different chromosomes segregate independently; statistically this means that SNPs on different chromosomes are conditionally independent given all markers in the genome. The latter explains that markers in a same chromosome tend to be inherited together during meiosis, which statistically implies that we expect an increased number of edges in the conditional independence graph between markers within a chromosome.

Figure 1(c) shows an example of an estimated conditional independent graph between markers. This graph includes 10 distinct sub-graphs, each of which corresponds to a linkage group. In this graph given all markers on a genome, markers within the linkage groups are conditionally dependent, *genetic linkage*, and markers between linkage groups are conditionally independent, due to the *independent assortment law*.

Some genotype studies suffer from low number of individuals or they contain signatures of epistatic selection (Behrouzi and Wit, 2017a) which may cause bias in determining the linkage groups. To address this problem beside the model selection step we use the fast-greedy algorithm to detect the communities (linkage groups) in the inferred graph. This community detection algorithm reflects the two mentioned biological concepts in a sense that it defines communities whose are highly connected inside a community and few links between communities.

### 3.3 Ordering markers

Assume that a set of  $d$  markers have been assigned to the same linkage group. Let  $G(V^{(d)}, E^{(d)})$  be a sub-graph on the set of unordered  $d$  markers, where  $V^{(d)} = \{1, \dots, d\}$ ,  $d \leq p$  and the edge set  $E^{(d)}$  represents the estimated edges among  $d$  markers where  $E^{(d)} \subseteq E$ . We remark that the precision matrix  $\widehat{\Theta}_\lambda^{(d)}$ , a submatrix of  $\widehat{\Theta}_\lambda$ , contains all conditional dependence relations between the set of  $d$  markers. Depending on the type of mating between the parental lines we introduce two methods to order markers, one based on dimensionality reduction and another based on bandwidth reduction. Both methods result in an one-dimension map.

**Inbred** In inbred populations, markers in the genome of the progenies can be assigned to their parental homologues resulting in a simpler conditional independence pattern between neighboring markers. In the case of inbreeding, we use multidimensional scaling (MDS). A metric MDS is a classical approach that maps the original high dimensional space to a lower dimensional space, while attempting to maintain pairwise distances. We define the distance matrix as  $D = -\log(\rho)$ , which is a  $d \times d$  symmetric matrix where  $D_{ii} = 0$  and  $D_{ij} \geq 0$ ,  $i \neq j$ . Here, the matrix  $\rho$  represents the conditional correlation among  $d$  objects which can be obtained as  $\rho_{ij} = -\frac{\theta_{ij}}{\sqrt{\theta_{ii}}\sqrt{\theta_{jj}}}$ , where  $\theta_{ij}$  is the  $ij$ -th element of the precision matrix  $\Theta$ .

We aim to construct a configuration of  $d$  data points in a one dimensional Euclidean space by using information about the distances between the  $d$  nodes. Given the distance matrix  $D$ , we define a linear ordering  $L$  of  $d$  elements such that the distance  $\widehat{D}$  between them is similar to  $D$ . We consider a metric MDS, which minimizes  $\widehat{L} = \arg \min_L \sum_{i=1}^d \sum_{j=1}^d (D_{ij} - \widehat{D}_{ij})^2$  across all linear ordering.

**Outbred** An outbred population derived from mating two non-homozygous parents result in markers in the genome of progenies that can not be easily assigned to their parental homologues. Neighboring markers that vary only on different haploids will appear as independent, which therefore requires a different ordering algorithm [see Figure 2c]. In that case, we use the reverse Cuthill-McKee (RCM) algorithm (Cuthill and McKee, 1969) to order markers. This algorithm is based on graph models. It reduces the bandwidth of the associated adjacency matrix,  $A_{d \times d}$ , for the sparse matrix  $\widehat{\Theta}_\lambda^{(d)}$ . The bandwidth of the matrix  $A$  is defined by  $\beta = \max_{\theta_{ij} \neq 0} |i - j|$ . The RCM algorithm produces a permutation matrix  $P$  such that  $PAP^T$  has a smaller bandwidth than  $A$  does. The bandwidth is decreased by moving the non-zero elements of the matrix  $A$  closer to the main diagonal. The way that the non-zero elements should be moved is decided by relabeling the nodes in graph  $G(V_d, E_d)$  in consecutive order. Moreover, all of the nonzero elements are clustered near the main diagonal.

## 4 Simulation study

In this section, we study the performance of the proposed method for different diploids and polyploids. In section 4.1, we perform a comprehensive simulation study to compare the performance of the proposed method with commonly used tools in diploid map constructions, namely JOINMAP (Jansen et al., 2001) and MSTMap (Wu et al., 2008). The former is based on Monte Carlo maximum likelihood and the latter uses a minimum spanning tree of a graph.

In section 4.2 we report the performance of the proposed method on simulated tetraploids  $q = 4$  and hexaploids  $q = 6$ . At this moment the proposed method is the only method that construct linkage maps for polyploids automatically without any manual adjustment. Thus, we do not compare the proposed method with other methods in this case.

### 4.1 Diploid species

We simulate genotype data from an inbred  $F2$  population. This population type generates discrete random variables with values  $Y = \{0, 1, 2\}$  associated with the three distinct genotype states,  $AA$ ,  $Aa$ , and  $aa$  at each marker. The procedure in generating genotype data is as follows: First, two homozygous parental lines with genotypes  $AA$  and  $aa$  at each loci are simulated. A given number of markers,  $p$ , are spaced along the predefined chromosomes. Then, two parental lines are crossed to give an  $F1$  population with all heterozygous genotypes  $Aa$  at each marker location. Finally, a desired number of individuals,  $n$ , are simulated from the gametes produced by the  $F1$  population.

Genotyping error means the observed genotype for an individual is not necessarily identical to its true genotype. For example, observing genotype  $AA$  when  $Aa$  is the true genotype. Genotyping errors can distort the final genetic map especially by incorrectly ordering markers and inflating map length. Therefore, ordering markers that contain genotyping errors is an essential task in constructing high-quality linkage maps. To investigate this, we create genotyping errors in the simulated datasets [see supplementary materials] by randomly flipping the heterozygous loci along the chromosomes to either one of the homozygous. Also, missing observations are randomly inserted along chromosomes by simply deleting genotypes.

For each simulated data, we compare the performance of the map construction in netgwas with two other models: JOINMAP, MSTMap. We compute two criteria: grouping accuracy (GA) and ordering accuracy (OA) to assess the performance of the above mentioned tools in estimating correct map. The former, measures the closeness of the estimated number of linkage groups to the correct number of linkage groups, and latter calculates the ratio of markers that are correctly ordered. The grouping accuracy is defined as follows  $GA = \frac{1}{1 + (LG - \widehat{LG})^2}$ , where  $LG$  stands for actual

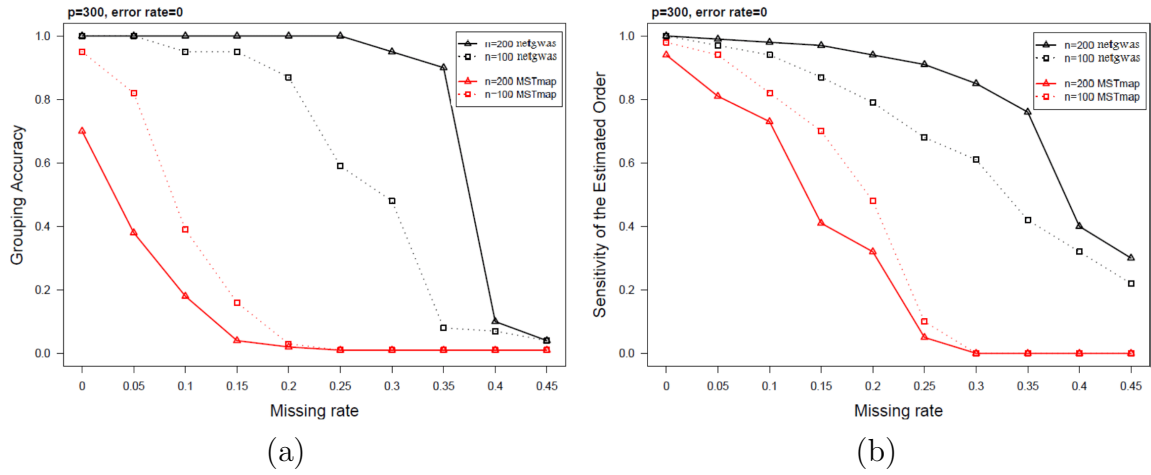


Figure 3: Performance comparison between map construction in netgwas and MSTMAP for different missingness rates with no genotyping errors. The variables  $p$  and  $n$  represent numbers of markers and individuals in the simulated diploid genotype datasets. (a) reports the grouping, and (b) shows ordering accuracy scores for 50 independent runs

number of linkage groups and  $\widehat{LG}$  is estimated number of linkage groups. The GA criteria is a positive value with maximum at 1. A high value of GA is indicator of a good performance in determining the correct number of linkage groups. To compute ordering accuracy, we calculate the Jaccard distance,  $d_J$ , which measures the mismatches between the estimated order and the true order. We define the ordering accuracy of the estimated map as  $OA = \frac{1}{1+d_J}$ . This measurement lies between 0 and 1, where 1 and 0 stand for a perfect and a bad ordering, respectively.

In terms of computation, netgwas runs in parallel. In the performed simulations, the map construction function in netgwas and the MSTMAP both were run on a Linux machine with 24 2.5 GHz Intel Xeon processors and 128 GB memory. JOINMAP only runs on Windows. It was run in a Windows machine with 3.20 GHz Intel Xeon processors and 8 GB RAM memory.

**Evaluation of estimated maps in presence of missing genotypes** We study the effect of different ratios of missingness in the accuracy of the estimated linkage maps using two methods: netgwas and MSTMAP. The simulated data contain 300 markers both for  $n = 100$  and  $n = 200$  individuals where the missingness rates range from 0 to 0.45. In this sets of simulations we assumed no genotyping error.

Figure 3 evaluates the accuracy of estimated maps in terms of grouping (Figure 3a) and ordering accuracies (Figure 3b). In general, this figure shows that netgwas constructs significantly better maps than MSTMAP across the full range of missingness

rates. More specifically, for moderate number of individuals, ( $n = 200$ ), Figure 3a shows that netgwas correctly estimates the actual number of linkage groups for missingness rates up to 0.25, and when rates lie between 0.25 and 0.35 netgwas estimates the actual number of linkage group with a high accuracy ( $\geq 0.90$ ). netgwas starts estimating the actual number of linkage groups poorly when the missing rate is higher than 0.35. For  $n = 100$  netgwas correctly estimates the actual number of linkage groups up to 0.05 missingness, and with high accuracy ( $\geq 0.9$ ) estimates the number of linkage groups for missingness rates between 0.05 and 0.2. For larger than 0.2 missingness the accuracy drops. MSTMAP estimates the actual number of linkage groups always significantly worse than netgwas. Its performance starts to drop immediately when there is some level of missingness. Surprisingly, it estimates the number of linkage groups better when  $n = 100$  than  $n = 200$ .

Figure 3b shows the ordering accuracy within each correctly estimated linkage group. Ordering quality in netgwas is significantly better than MSTMAP for both  $n = 100$  and  $n = 200$ . More specifically, when  $n = 100$  and missing rate equals zero netgwas orders markers perfectly (100% accuracy) and MSTMAP orders markers with a high accuracy (95%). In addition, when the missingness rates increase the map construction function in netgwas outperform the MSTMAP in ordering markers within each LG. Surprisingly, when the number of individual increases, MSTMAP performs worse in ordering markers.

## 4.2 Polyploid species

Here, we apply netgwas to simulated outbred polyploid genotype datasets. We use PedigreeSim (Voorrips and Maliepaard, 2012) to simulate  $F1$  mapping populations in tetraploids ( $q = 4$ ) and hexaploids ( $q = 6$ ) with  $n = 200$  individuals. PedigreeSim simulates polyploid genotypes with different configurations such as chromosomal pairing modes during meiosis. The simulated tetraploids ( $q = 4$ ) are motivated by autotetraploid potato where  $Y = \{0, 1, 2, 3, 4\}$  corresponds to the five biallelic tetraploid genotype states, ( $aaaa$ ,  $Aaaa$ ,  $AAaa$ ,  $AAAa$ ,  $AAAA$ ) which are created across 12 chromosomes. The simulated hexaploids ( $q = 6$ ) are motivated by allohexaploid peanut, a polyploid species that contains 10 chromosomes, where  $Y = \{0, 1, 2, 3, 4, 5, 6\}$  corresponds to the seven genotype states ( $aaaaaa$ ,  $Aaaaaa$ ,  $AAaaaa$ ,  $AAAaaa$ ,  $AAAAAa$ ,  $AAAAAA$ ) across its genome. In total, 50 populations each consisting of  $p = 1000$  markers were simulated for each scenario.

We use the mean square error (MSE) as a measure for evaluating the performance of the proposed method on detecting the true number of chromosomes. In the tetraploid simulation the mean of MSE was 0.52, and for the hexaploid simulation it was 0.15. Figure 4 shows the performance of the proposed method in ordering markers for tetraploids (Figure 4a) and hexaploids (Figure 4b). The solid line shows the median of estimated order of each marker across a chromosome versus the true

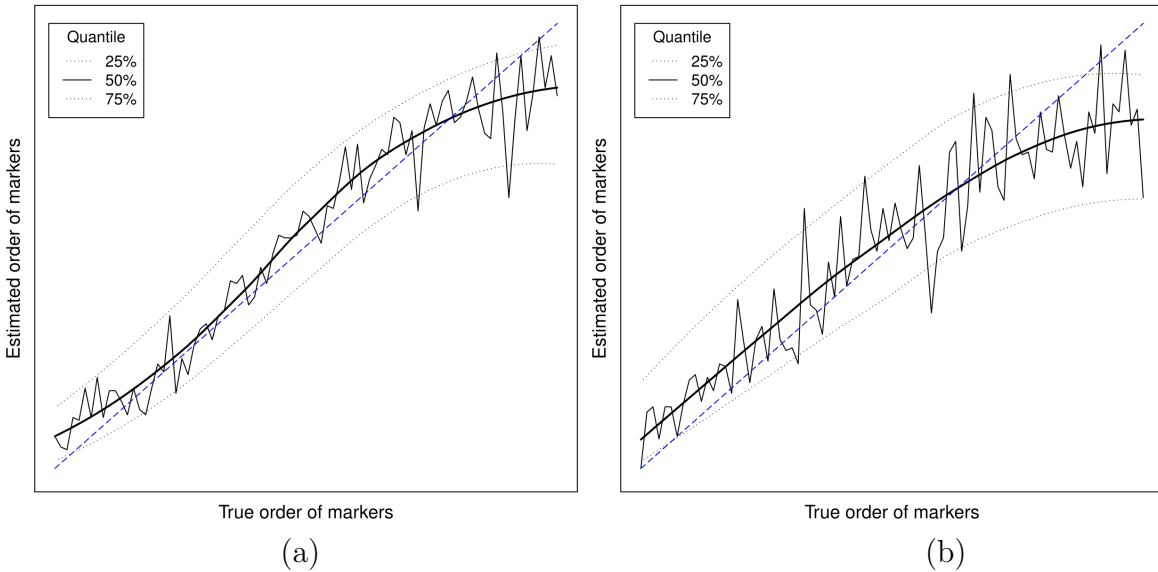


Figure 4: The performance of the netgwas on different polyploid simulated datasets. The median, lower quartile, and upper quartile of estimated order versus the true order for (a) tetraploids ( $q = 4$ ), and (b) hexaploid simulated datasets ( $q = 6$ ). The solid lines are the median and the smoothed median. The blue dashed line shows the ideal ordering.

order, and the lower (25%) and the upper quartiles (75%) of estimated markers order is shown as dashed lines. This Figure shows that although ordering markers in outcrossing families is challenging [see section 2.3], but the proposed method orders markers reasonably well.

## 5 Construction of linkage map for barley

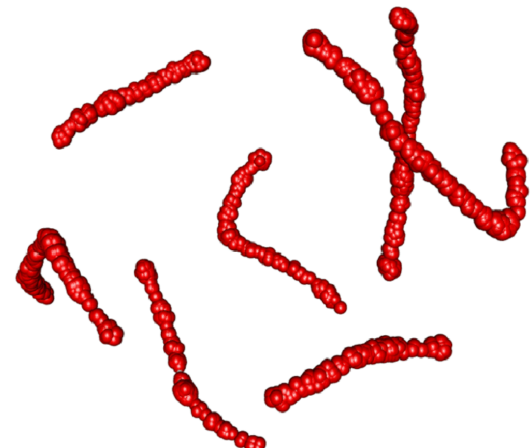
A barley genotyping dataset is used in the literature to compare different map construction methods for real-world diploid data. This genotyping dataset is generated from a doubled haploid population which allows to achieve homozygous individuals,  $Y = \{0, 1\}$ . Barley genotype data is the result of crossing Oregon Wolfe Barley Dominant with Oregon Wolfe Barley Recessive (see <http://wheat.pw.usda.gov/ggpages/maps/OWB>). The Oregon Wolfe Barley (OWB) data includes  $p = 1328$  markers that were genotyped on  $n = 175$  individuals which 0.02% genotypes are missing. The barley dataset is expected to yield 7 linkage groups, one for each of the 7 barley chromosomes.

As shown in Figure 5, through estimating  $\hat{\Theta}_\lambda$ , which contains conditional (in)dependence relationships between barley markers, we are able to correctly detect the 7 barley chromosomes as sub-graphs in the estimated undirected graph. Furthermore, using the

Estimated number of linkage groups (LGs) for OWB data set		
	Estimated # LG	Size of the LGs
netgwas	<b>7</b>	<b>140, 199, 211, 187, 236, 182, 173</b>
MSTMap	1	1328

Comparison of ordering accuracy between netgwas and MSTMap. In this Table assumed MSTMAP has estimated correctly the number of LGs in the OWB data set.

Linkage Group (LG)	Sensitivity Score	
	netgwas	MSTMap
1	0.86	<b>0.96</b>
2	<b>0.78</b>	0.52
3	0.78	<b>0.92</b>
4	<b>0.74</b>	0.49
5	<b>0.71</b>	0.38
6	<b>0.61</b>	0.50
7	<b>0.70</b>	0.61
Average	<b>0.74</b>	0.63



Estimated linkage map for barley using netgwas

Figure 5: Summary of comparison between netgwas and MSTMap in the barely data. This Table summarizes the estimated number of LGs (chromosomes) and size of markers within each LGs. Also, at the bottom it shows the average ordering accuracy scores for the two methods. The right Figure shows the estimated undirected graph in netgwas for the barley data. It consists of 7 sub-graphs, each of which shows a chromosome.

conditional correlation matrix as distance in the multi-dimensional scaling approach helps us to order markers with high accuracy. In addition, Figure 5 reports the result of applying the two methods netgwas and MSTMap to construct linkage map for the barley data. The top part of Figure 5 shows that our method estimates the true number of chromosomes correctly. Also, the size of markers within each chromosome is consistent with the number of markers that has been reported in Cistué et al. (2011). MSTMap was not able to estimate the true number of chromosomes and grouped all 1328 markers as one linkage group. The bottom of Figure 5 shows the accuracy of estimated markers order in 7 barley chromosomes. To be able to compare markers order in both methods we used the actual map to cluster markers in map resulted from MSTMap. Thus, in the bottom of Figure 5 is assumed that the MSTMap has estimated the correct number of chromosomes. Average ordering accuracy scores across the linkage groups in netgwas is higher than those in MSTMap except in chromosomes 1 and 3.

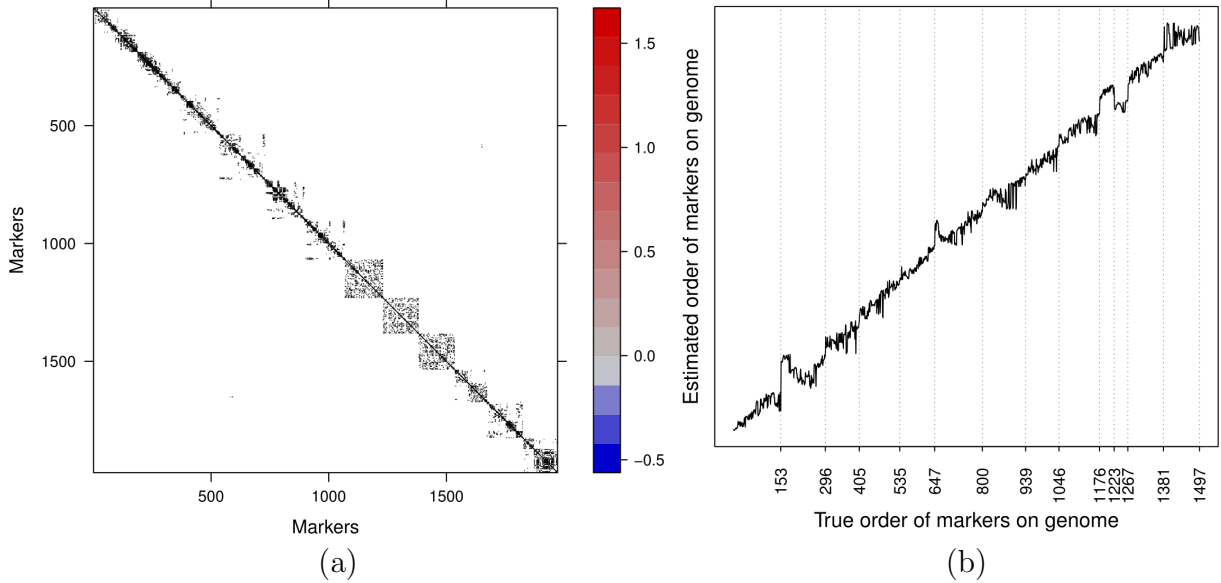


Figure 6: Construction linkage map in potato. (a) represent the estimated precision matrix for the unordered genotype data of tetraploid potato. (b) shows the true order of markers across potato genome versus the estimated order. Each dashed line represents a chromosome. All the potato chromosomes are detected correctly only chromosome 10, markers between 1176 and 1267, is detected as two linkage groups.

## 6 Construction of linkage map for tetraploid potato

World-wide, potato is the third most important food crop. However, the complex genetic structure of tetraploid potato's (*Solanum tuberosum* L.) makes it difficult to improve important traits such as disease resistance in this crop. Thus, there is a great interest to construct linkage maps in potato to identify markers related to disease resistance genes.

The full-sib mapping population MSL603 consists of 156 F1 plants resulting from a cross between female parent “Jacqueline Lee” and the male parent “MSG227-2”. The obtained genotype data contains 1972 SNP markers (Massa et al., 2015) with five allele dosages which are associated with the random variables  $Y_j \in \{0, 1, \dots, 4\}$  for  $j = 1, \dots, 1972$ .

Figure 6 represents the result of employing the proposed map construction method to the unordered potato genotype data. Figure 6a shows the estimated sparse precision matrix which reveals the number of potato chromosomes as blocks across the diagonal. The potato genome contains 12 chromosomes. The proposed method has estimated 13, where it detects chromosome 10 as two linkage groups, as can be seen in the diagonal of the precision matrix: markers between locus 1176 and 1267 belong to the same chromosome. Figure 6b compares the estimated order versus the true order

of markers. Each dashed line shows the estimated linkage groups. Markers ordered reasonably fine, given that ordering markers always have been a challenging task in linkage map constructions in particular for polyploid species.

## 7 Conclusion

Construction of linkage maps is a fundamental step required in a detailed genetic study of diseases and traits. A high-quality linkage map provides opportunities for higher throughput gene manipulation and phenotype improvement.

Diploid species contain two, and polyploids contain more than two copies of chromosomes. If a location in a chromosome, genetic marker, be identical for the all copies of a chromosome the SNP marker is in the homozygous state, and in heterozygous state otherwise. A marker can be in  $q + 1$  genotype state in a heterozygous population, where the random variable  $Y$  takes on a finite number of values  $\{0, 1, \dots, q\}$ , where  $q$  presents the ploidy level.

Here we introduced a novel method to construct linkage maps from high-throughput genotype data where the number of genetic markers exceed the number of individuals. The proposed method constructs a linkage map for any biparental diploid or polyploid population. We propose to build linkage maps in two steps. (i) revealing conditional independence relationships between markers on the genome, (ii) ordering markers in each linkage group, typically a chromosome. In the first step of the proposed method, we used the Markov properties of adjacent markers: the genotype of an individual haploid at marker  $Y_j$  given its genotype at  $Y_{j-1}$  or  $Y_{j+1}$  is conditionally independent of genotype at any other marker location. This property defines a graphical model for discrete random variables.

Here, we introduce a Gaussian copula graphical model, where we employs a penalized EM algorithm to estimate a sparse precision matrix  $\hat{\Theta}_\lambda$ . This method iteratively computes the conditional expectation of the complete penalized log-likelihood, and optimizes this to estimate  $\hat{\Theta}_\lambda$ . This method can deal with missing values which is very routine in many genotype datasets. The nonparanormal skeptic is an alternative approach [discussed in supplementary materials], which is computationally faster but can not deal with missing values. Depending on the type of mapping population, inbred or outbred, in step 2 of the proposed linkage map construction we use either a multi-dimensional scaling approach or the Cuthill-McKee algorithm. Both ordering algorithms result in an one-dimensional map. We note that in outcrossing populations, ordering markers is a difficult task due to the lack of a clear definition of the parental.

We performed several simulation studies to compare the performance of the proposed method with other commonly used diploid map construction tools. To address the challenges in the construction of a linkage map from real-world data, we study the

performance of the proposed method on simulated data with high ratios of missingness and genotyping error. Based on our simulation studies, the netgwas outperforms the commonly used available tools, either when the input data is clean with no missing observation and when the input data is noisy and incomplete.

As outlined in Cervantes-Flores et al. (2008), constructing linkage maps in polyploids, with outcrossing behavior, is a challenging task. So far, based on our experience, no method has been developed to construct polyploid linkage maps for a large number of different marker types without any manual adjustment and visual inspection. Based on the simulated polyploids with outcrossing behavior, the proposed method detects the true number of linkage groups with high accuracy, and orders marker reasonably well.

We implemented the proposed method to two real-world genotype datasets, namely barley and potato. In barley map construction, we detected correctly its 7 chromosomes, whereas the other method groups all the markers as one linkage group. The netgwas orders marker with higher accuracy in most of the chromosomes except in two cases that the other method have better ordering quality. The proposed method detects all the potato chromosomes, although it identifies chromosome 10 as two linkage groups. It orders markers within each chromosome with a reasonable quality. We remark that the proposed map construction method uses all possible marker types unlike the other map construction methods that use a subset of markers e.g. where both parents were heterozygous (Grandke et al., 2017).

Overall, construction diploids and polyploids linkage maps using graphical models provides an efficient way for constructing high-density and high-quality linkage maps, even for noisy and incomplete data.

We remark that netgwas works also for multiallelic loci which are locations in a genome that contain three or more observed alleles. For example, assume that A, T, and G are three possible alleles at location  $j$  on genome, unlike the most usual cases that only two alleles in a location can be observed (e.g. A and G). We propose to analyze a dataset containing multiallelic loci separately, or analyze them jointly. In the former case, observed alleles counts once as reference, and therefore allowing for one separate dataset. In the above example three datasets will be generated: first dataset counts number of A as a reference allele, second dataset counts number of T as a reference allele, and the third dataset G allele is considered as reference. Each dataset can be analyzed separately, and to control similarity between the estimated precision matrices the fused graphical lasso can be used. The final map can be obtained through ordering markers in an estimated precision matrix. In the latter case, in the above example, we combine all the three datasets as one dataset in such a way that it creates three replicates of  $n \times p$  dimension. Moreover, we analyze the obtained dataset and construct final linkage map.

Once we have the linkage map, one interesting question is detecting epistatic interactions, and intra- and inter-chromosomal interactions along genome[See Behrouzi

and Wit, (2017a)].

## Supplementary Materials

### Computing conditional expectation

We calculate  $\bar{R}$  in equation (6) of the paper as

$$E\left[Z^{(i)}Z^{(i)t}|Y^{(i)}, \widehat{\Theta}^{(m)}\right] = E\left[Z^{(i)}|Y^{(i)}, \widehat{\Theta}^{(m)}\right]E\left[Z^{(i)}|Y^{(i)}, \widehat{\Theta}^{(m)}\right]^t + cov\left[Z^{(i)}|Y^{(i)}, \widehat{\Theta}^{(m)}\right] \quad (8)$$

The conditional random variable  $Z|Y$  follows a truncated p-variate normal distribution. Wilhelm and Manjunath (2010) provided the analytical solution to compute moments of truncated multivariate normal distribution. However, their approach is feasible for only very few variables. Here, rather we propose to simulate a large number of samples from the truncated p-variate normal distribution and compute the sample conditional covariance matrix and sample conditional mean to estimate  $E\left[Z^{(i)}Z^{(i)t}|Y^{(i)}, \widehat{\Theta}^{(m)}\right]$  using the equation (8).

Alternatively, we use an efficient approximate estimation algorithm which is implemented in Behrouzi and Wit, (2017a). The variance elements in the conditional expectation matrix can be calculated through the second moment of the conditional  $Z_j^{(i)}|Y^{(i)}$ , and the rest of the elements in this matrix can be approximated through  $E(Z_j^{(i)}Z_{j'}^{(i)}|y^{(i)}; \widehat{\Theta}, \widehat{\mathcal{D}}) \approx E(Z_j^{(i)}|y^{(i)}; \widehat{\Theta}, \widehat{\mathcal{D}})E(Z_{j'}^{(i)}|y^{(i)}; \widehat{\Theta}, \widehat{\mathcal{D}})$  using mean field theory. The first and second moment of  $z_j^{(i)}|y^{(i)}$  can be written as

$$E(Z_j^{(i)}|y^{(i)}, \widehat{\Theta}, \widehat{\mathcal{D}}) = E[E(Z_j^{(i)}|z_{-j}^{(i)}, y_j^{(i)}, \widehat{\Theta}, \widehat{\mathcal{D}})|y^{(i)}, \widehat{\Theta}, \widehat{\mathcal{D}}], \quad (9)$$

$$E((Z_j^{(i)})^2|y^{(i)}, \widehat{\Theta}, \widehat{\mathcal{D}}) = E[E((Z_j^{(i)})^2|z_{-j}^{(i)}, y_j^{(i)}, \widehat{\Theta}, \widehat{\mathcal{D}})|y^{(i)}, \widehat{\Theta}, \widehat{\mathcal{D}}], \quad (10)$$

where  $z_{-j}^{(i)} = (z_1^{(i)}, \dots, z_{j-1}^{(i)}, z_{j+1}^{(i)}, \dots, z_p^{(i)})$ . The inner expectations in (9) and (10) are relatively straightforward to calculate.  $z_j^{(i)}|z_{-j}^{(i)}, y_j^{(i)}$  follows a truncated Gaussian distribution on the interval  $[c_{y_j^{(i)}}^{(j)}, c_{y_j^{(i)}+1}^{(j)}]$  with parameters  $\mu_{i,j}$  and  $\sigma_{i,j}^2$  given by

$$\mu_{ij} = \widehat{\Sigma}_{j,-j}\widehat{\Sigma}_{-j,-j}^{-1}z_{-j}^{(i)t},$$

$$\sigma_{i,j}^2 = 1 - \widehat{\Sigma}_{j,-j}\widehat{\Sigma}_{-j,-j}^{-1}\widehat{\Sigma}_{-j,-j}.$$

Let  $r_{k,l} = \frac{1}{n} \sum_{i=1}^n E(Z_k^{(i)}Z_l^{(i)}|y^{(i)}, \widehat{\Theta}, \widehat{\mathcal{D}})$  be the  $(k,l)$ -th element of empirical correlation matrix  $\bar{R}$ , then to obtain the  $\bar{R}$  two simplifications are required.

$$\begin{aligned} E(Z_k^{(i)}Z_l^{(i)t}|y^{(i)}, \widehat{\Theta}, \widehat{\mathcal{D}}) &\approx E(Z_k^{(i)}|y^{(i)}, \widehat{\Theta}, \widehat{\mathcal{D}})E(Z_l^{(i)}|y^{(i)}, \widehat{\Theta}, \widehat{\mathcal{D}}) & \text{if } 1 \leq k \neq l \leq p, \\ E(Z_k^{(i)}Z_l^{(i)t}|y^{(i)}, \widehat{\Theta}, \widehat{\mathcal{D}}) &= E((Z_k^{(i)})^2|y^{(i)}, \widehat{\Theta}, \widehat{\mathcal{D}}) & \text{if } k = l. \end{aligned}$$

Applying the results in the appendix to the conditional  $z_j^{(i)} \mid z_{-j}^{(i)}, y_j^{(i)}$  we obtain

$$E(Z_j^{(i)} \mid y^{(i)}; \widehat{\Theta}, \widehat{\mathcal{D}}) = \widehat{\Sigma}_{j,-j} \widehat{\Sigma}_{-j,-j}^{-1} E(Z_{-j}^{(i)t} \mid y^{(i)}; \widehat{\Theta}, \widehat{\mathcal{D}}) + \frac{\phi(\tilde{\delta}_{j,y_j^{(i)}}^{(i)} - \phi(\tilde{\delta}_{j,y_j^{(i)}+1}^{(i)}))}{\Phi(\tilde{\delta}_{j,y_j^{(i)}}^{(i)}) - \Phi(\tilde{\delta}_{j,y_j^{(i)}+1}^{(i)})} \tilde{\sigma}_j^{(i)}, \quad (11)$$

$$\begin{aligned} E((Z_j^{(i)})^2 \mid y^{(i)}; \widehat{\Theta}, \widehat{\mathcal{D}}) &= \widehat{\Sigma}_{j,-j} \widehat{\Sigma}_{-j,-j}^{-1} E(Z_{-j}^{(i)t} Z_{-j}^{(i)} \mid y^{(i)}; \widehat{\Theta}, \widehat{\mathcal{D}}) \widehat{\Sigma}_{-j,-j}^{-1} \widehat{\Sigma}_{j,-j}^t + (\tilde{\sigma}_j^{(i)})^2 \\ &+ 2 \frac{\phi(\tilde{\delta}_{j,y_j^{(i)}}^{(i)}) - \phi(\tilde{\delta}_{j,y_j^{(i)}+1}^{(i)})}{\Phi(\tilde{\delta}_{j,y_j^{(i)}+1}^{(i)}) - \Phi(\tilde{\delta}_{j,y_j^{(i)}}^{(i)})} [\widehat{\Sigma}_{j,-j} \widehat{\Sigma}_{-j,-j}^{-1} E(Z_{-j}^{(i)t} \mid y^{(i)}; \widehat{\Theta}, \widehat{\mathcal{D}})] \tilde{\sigma}_j^{(i)} \\ &+ \frac{\delta_{j,y_j^{(i)}}^{(i)} \phi(\tilde{\delta}_{j,y_j^{(i)}}^{(i)}) - \tilde{\delta}_{j,y_j^{(i)}+1}^{(i)} \phi(\tilde{\delta}_{j,y_j^{(i)}+1}^{(i)})}{\Phi(\tilde{\delta}_{j,y_j^{(i)}+1}^{(i)}) - \Phi(\tilde{\delta}_{j,y_j^{(i)}}^{(i)})} (\tilde{\sigma}_j^{(i)})^2, \end{aligned} \quad (12)$$

where  $Z_{-j}^{(i)} = (Z_1^{(i)}, \dots, Z_{j-1}^{(i)}, Z_{j+1}^{(i)}, \dots, Z_p^{(i)})$  and  $\tilde{\delta}_{j,y_j^{(i)}}^{(i)} = [c_j^{(i)} - E(\tilde{\mu}_{ij} \mid y^{(i)}; \widehat{\Theta}, \widehat{\mathcal{D}})] / \tilde{\sigma}_{ij}$ .

In this way, an approximation for  $\bar{R}$  is obtained as follows:

$$\tilde{r}_{kl} = \begin{cases} \frac{1}{n} \sum_{i=1}^{i=n} E(Z_k^{(i)} \mid y^{(i)}, \widehat{\Theta}^{(m)}, \widehat{\mathcal{D}}) E(Z_l^{(i)} \mid y^{(i)}, \widehat{\Theta}^{(m)}, \widehat{\mathcal{D}}) & \text{if } 1 \leq k \neq l \leq p \\ \frac{1}{n} \sum_{i=1}^{i=n} E((Z_k^{(i)})^2 \mid y^{(i)}, \widehat{\Theta}^{(m)}, \widehat{\mathcal{D}}) & \text{if } k = l. \end{cases}$$

The latent graphical model discussed in the paper, though it is a natural approach, is computationally expensive for a big number of variables ( $p > 2000$ ). Alternatively, here we explain an alternative method to construct high-dimensional undirected graphical model.

## Nonparanormal SKEPTIC

Alternatively, we use the nonparanormal skeptic approach (Liu et al., 2012) to estimate the penalized concentration matrix  $\Theta$ . In this approach, instead of using the transformed data to estimate precision matrix  $\Theta$ , a sample correlation matrix  $\Gamma$  can be computed from pairwise rank correlations, such as Kendall's tau and Spearman's rho. For the random vector  $y_j^{(1)}, \dots, y_j^{(n)}$  the Kendall's tau and Spearman's rho are given, respectively, by

$$\widehat{\tau}_{jl} = \frac{2}{n(n-1)} \sum_{i,i=1}^n \text{sign}(y_j^{(i)} - y_j^{(i)})(y_l^{(i)} - y_l^{(i)})$$

and

$$\hat{\rho}_{jl} = \frac{\sum_{i=1}^n (r_j^i - \bar{r}_j)(r_l^i - \bar{r}_l)}{\sqrt{\sum_{i=1}^n (r_j^i - \bar{r}_j)^2} \cdot \sqrt{\sum_{i=1}^n (r_l^i - \bar{r}_l)^2}}$$

$$\hat{\Gamma}_{jl} = \begin{cases} \sin(\frac{\pi}{2}\hat{\tau}_{jl}) & j \neq l \\ 1 & j = l \end{cases} ; \quad \hat{\Gamma}_{jl} = \begin{cases} 2 \sin(\frac{\pi}{6}\hat{\rho}_{jl}) & j \neq l \\ 1 & j = l. \end{cases}$$

To estimate the sparse precision matrix and the graph, one can use either the graphical lasso

$$\hat{\Theta}_{\text{glasso}} = \arg \max_{\Theta} \left\{ \log |\Theta| - \text{tr}(\Gamma \Theta) - \lambda \|\Theta\|_1 \right\} \quad (13)$$

or CLIME estimator, with  $\hat{\Gamma}$  as input

$$\hat{\Theta}_{\text{CLIME}} = \arg \min_{\Theta} \|\Theta\|_1 \quad \text{subject to} \quad \|\hat{\Gamma}\Theta - I_p\|_{\infty} \leq \lambda, \quad (14)$$

Both methods involve convex optimization problems, which can be solved efficiently.

## Simulation study

### Evaluation of estimated maps in presence of genotyping errors

We study the accuracy of the estimated linkage maps when genotyping errors are randomly distributed across the genetic markers. The simulated data contain a ratio of "bad markers" ranging from 0 up to 0.45 genotyping errors. We activated the error-detection feature in MSTMAP. Figure 7a shows that when datasets contain genotyping errors, netgwas perfectly estimates the correct number of LGs in particular when the sample size is sufficient,  $n > 100$ . In addition, the quality of estimated linkage maps – in terms of estimating the actual number of LGs and markers ordering – is significantly better in the netgwas than those in the MSTMAP, even with its error-detection feature activated.

Based on our simulations, we remark that both netgwas and MSTMAP keep erroneous markers in the estimated linkage map. However, netgwas orders them correctly in the right LG (see Figure 7), whereas MSTMAP performs poorly, in comparison to netgwas, in detecting LGs as well as ordering markers correctly.

In general for moderate number of individuals, when data contains genotyping errors the netgwas constructs a linkage map that is very close to the actual map, both in terms of accuracy of the estimated linkage groups and the ordering accuracy. This is due to the fact that conditional independence is an effective way to recover relationships among genetic markers.

Table 2

Summary of performance measures of linkage map construction in simulated F2 populations for netgwas, MSTMAP and JOINMAP at different rates of missingness and genotyping errors. The Tables presents the grouping and the ordering accuracy scores for 50 independent runs and standard deviation in parentheses. Best scores are boldfaced.

Missing rate	Error rate	Grouping Accuracy			Ordering Accuracy		
		netgwas	MSTMap	JOINMAP	netgwas	MSTMap	JOINMAP
<b>p=300 &amp; n=200</b>							
0	0	<b>1.00</b> (0.00)	0.70 (0.12)	0.00 (0.00)	<b>1.00</b> (0.00)	0.94 (0.00)	0.00 (0.00)
0.05	0.05	<b>1.00</b> (0.00)	0.30 (0.19)	0.00 (0.00)	<b>0.91</b> (0.03)	0.77 (0.11)	0.00 (0.00)
0.10	0.10	<b>1.00</b> (0.00)	0.04 (0.03)	0.00 (0.00)	<b>0.73</b> (0.03)	0.46 (0.26)	0.00 (0.00)
0.15	0.15	<b>1.00</b> (0.01)	0.01 (0.00)	0.00 (0.00)	<b>0.65</b> (0.04)	0.00 (0.00)	0.00 (0.00)
0.20	0.20	<b>1.00</b> (0.00)	0.01 (0.00)	0.00 (0.00)	<b>0.59</b> (0.02)	0.00 (0.00)	0.00 (0.00)
0.25	0.25	<b>0.95</b> (0.16)	0.01 (0.00)	0.00 (0.00)	<b>0.53</b> (0.03)	0.00 (0.00)	0.00 (0.00)
<b>p=500 &amp; n=200</b>							
0	0	<b>1.00</b> (0.00)	0.55 (0.34)	0.00 (0.00)	<b>1.00</b> (0.00)	0.90 (0.09)	0.00 (0.00)
0.05	0.05	<b>1.00</b> (0.00)	0.10 (0.07)	0.00 (0.00)	<b>0.77</b> (0.04)	0.61 (0.12)	0.00 (0.00)
0.10	0.10	<b>1.00</b> (0.00)	0.01 (0.00)	0.00 (0.00)	<b>0.60</b> (0.03)	0.18 (0.23)	0.00 (0.00)
0.15	0.15	<b>1.00</b> (0.00)	0.01 (0.00)	0.00 (0.00)	<b>0.56</b> (0.01)	0.00 (0.00)	0.00 (0.00)
0.20	0.20	<b>0.95</b> (0.16)	0.01 (0.00)	0.00 (0.00)	<b>0.54</b> (0.01)	0.00 (0.00)	0.00 (0.00)
0.25	0.25	<b>0.90</b> (0.21)	0.01 (0.00)	0.00 (0.00)	<b>0.51</b> (0.03)	0.00 (0.00)	0.00 (0.00)
<b>p=1000 &amp; n=200</b>							
0	0	<b>1.00</b> (0.00)	0.61 (0.36)	0.00 (0.00)	<b>1.00</b> (0.00)	0.91 (0.06)	0.00 (0.00)
0.05	0.05	<b>1.00</b> (0.00)	0.04 (0.03)	0.00 (0.00)	<b>0.56</b> (0.00)	0.51 (0.09)	0.00 (0.00)
0.10	0.10	<b>1.00</b> (0.00)	0.44 (0.16)	0.00 (0.00)	0.52 (0.00)	<b>0.78</b> (0.02)	0.00 (0.00)
0.15	0.15	<b>1.00</b> (0.01)	0.05 (0.00)	0.00 (0.00)	<b>0.52</b> (0.00)	0.60 (0.13)	0.00 (0.00)
0.20	0.20	<b>0.95</b> (0.14)	0.01 (0.00)	0.00 (0.00)	<b>0.51</b> (0.00)	0.00 (0.00)	0.00 (0.00)
0.25	0.25	<b>0.95</b> (0.14)	0.01 (0.00)	0.00 (0.00)	<b>0.51</b> (0.00)	0.00 (0.00)	0.00 (0.00)
<b>p=300 &amp; n=100</b>							
0	0	<b>1.00</b> (0.00)	0.70 (0.12)	0.00 (0.00)	<b>1.00</b> (0.00)	0.94 (0.00)	0.00 (0.00)
0.05	0.05	<b>0.95</b> (0.16)	0.82 (0.30)	0.00 (0.00)	0.76 (0.06)	<b>0.94</b> (0.09)	0.00 (0.00)
0.10	0.10	<b>1.00</b> (0.00)	0.31 (0.31)	0.00 (0.00)	<b>0.64</b> (0.05)	<b>0.64</b> (0.07)	0.00 (0.00)
0.15	0.15	<b>0.90</b> (0.21)	0.02 (0.01)	0.00 (0.00)	<b>0.56</b> (0.07)	0.24 (0.18)	0.00 (0.00)
0.20	0.20	<b>0.40</b> (0.44)	0.01 (0.00)	0.00 (0.00)	<b>0.45</b> (0.10)	0.00 (0.00)	0.00 (0.00)
0.25	0.25	<b>0.40</b> (0.35)	0.01 (0.00)	0.00 (0.00)	<b>0.38</b> (0.11)	0.00 (0.00)	0.00 (0.00)
<b>p=500 &amp; n=100</b>							
0	0	<b>1.00</b> (0.00)	0.80 (0.26)	0.00 (0.00)	<b>1.00</b> (0.00)	0.93 (0.05)	0.00 (0.00)
0.05	0.05	<b>1.00</b> (0.00)	0.34 (0.29)	0.00 (0.00)	0.62 (0.01)	<b>0.67</b> (0.10)	0.00 (0.00)
0.10	0.10	<b>1.00</b> (0.00)	0.08 (0.07)	0.00 (0.00)	<b>0.55</b> (0.02)	0.41 (0.08)	0.00 (0.00)
0.15	0.15	<b>0.87</b> (0.28)	0.05 (0.00)	0.00 (0.00)	0.50 (0.10)	<b>0.60</b> (0.13)	0.00 (0.00)
0.20	0.20	<b>0.51</b> (0.37)	0.01 (0.00)	0.00 (0.00)	<b>0.50</b> (0.07)	0.00 (0.00)	0.00 (0.00)
0.25	0.25	<b>0.21</b> (0.31)	0.01 (0.00)	0.00 (0.00)	<b>0.46</b> (0.16)	0.00 (0.00)	0.00 (0.00)
<b>p=1000 &amp; n=100</b>							
0	0	<b>1.00</b> (0.00)	0.74 (0.35)	0.00 (0.00)	<b>1.00</b> (0.00)	0.82 (0.08)	0.00 (0.00)
0.05	0.05	<b>1.00</b> (0.00)	0.13 (0.07)	0.00 (0.00)	<b>0.53</b> (0.01)	0.50 (0.04)	0.00 (0.00)
0.10	0.10	<b>0.95</b> (0.16)	0.01 (0.00)	0.00 (0.00)	<b>0.52</b> (0.01)	0.13 (0.16)	0.00 (0.00)
0.15	0.15	<b>0.95</b> (0.15)	0.00 (0.00)	0.00 (0.00)	<b>0.49</b> (0.04)	0.00 (0.00)	0.00 (0.00)
0.20	0.20	<b>0.85</b> (0.24)	0.00 (0.00)	0.00 (0.00)	<b>0.46</b> (0.07)	0.00 (0.00)	0.00 (0.00)
0.25	0.25	<b>0.82</b> (0.30)	0.00 (0.00)	0.00 (0.00)	<b>0.44</b> (0.05)	0.00 (0.00)	0.00 (0.00)

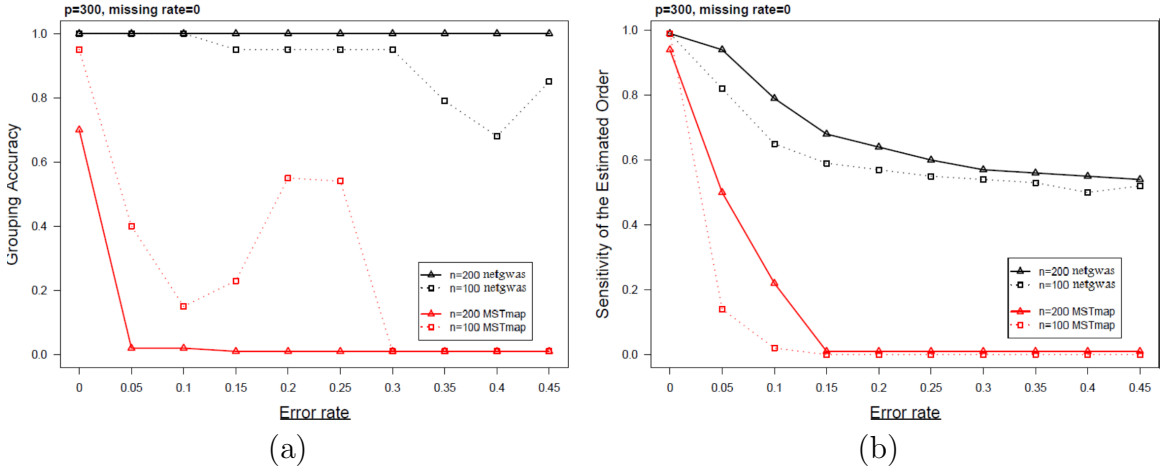


Figure 7: Genotyping errors randomly distributed over genetic markers: comparison between map construction in netgwas and MSTMAP in presence of different choices of the error rates and no missing data. (a) reports the grouping, and (b) shows ordering accuracy scores for 50 independent runs.

### Evaluation of estimated maps for incomplete and noisy data

The ordering accuracy scores in Table 2 should be interpreted carefully, as inversion in the order of flanking markers reduces the number of correct ordering and ultimately decreases orderings accuracy scores. In all scenarios, the proposed method detects linkage groups with higher accuracy. Furthermore, the netgwas performs well in correctly ordering markers as its ordering accuracy scores are higher compared to the other two methods, except in a few cases where MSTMAP performs better. Overall, given the various ratios of noisy and incomplete data netgwas estimates genetic linkage with higher accuracy compared to the other two methods.

Finally, we remark that determining linkage groups in JoinMAP requires an input parameter to be specified by the user, thereby influencing its output. However, our proposed method does not depend on any manual threshold or manually determining the linkage groups.

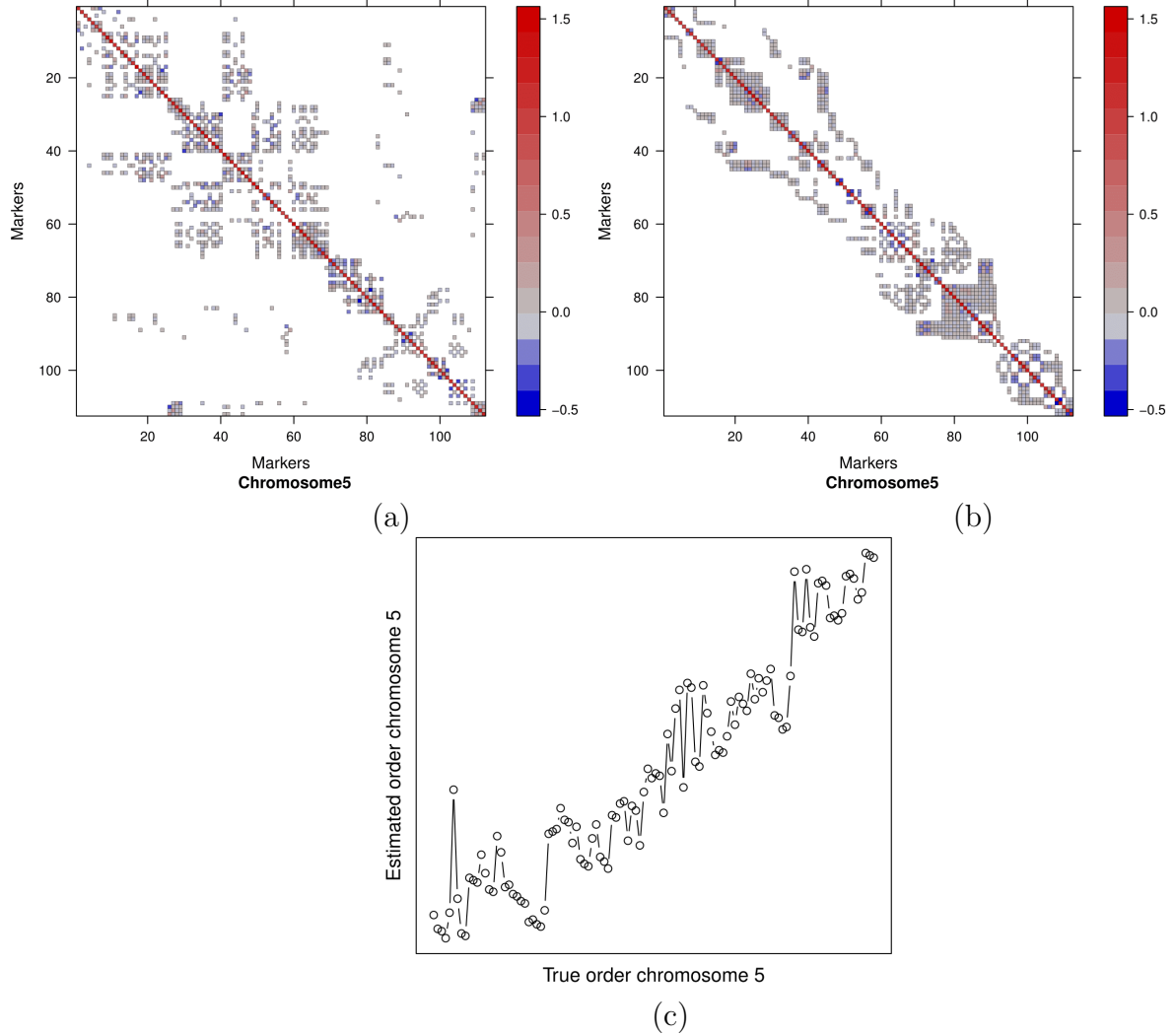


Figure 8: Visualizing the bandwidth reduction ordering algorithm in chromosome 5 of potato. (a) shows the estimated concentration sub-matrix for chromosome 5, (b) represents the result of performing reverse Cuthill-McKee algorithm on (a), (c) evaluates the estimated order resulted from (b) versus the true order for chromosome 5 in potato.

## References

- Broman, K. W., H. Wu, S. Sen, and G. A. Churchill (2003). R/qtl: Qtl mapping in experimental crosses. *Bioinformatics* 19(7), 889–890.
- Cai, T., W. Liu, and X. Luo (2011). A constrained l1 minimization approach to sparse precision matrix estimation. *Journal of the American Statistical Association*

tion 106(494), 594–607.

- Cervantes-Flores, J. C., G. C. Yencho, A. Kriegner, K. V. Pecota, M. A. Faulk, R. O. Mwanga, and B. R. Sosinski (2008). Development of a genetic linkage map and identification of homologous linkage groups in sweetpotato using multiple-dose aflp markers. *Molecular Breeding* 21(4), 511–532.
- Cistué, L., A. Cuesta-Marcos, S. Chao, B. Echávarri, Y. Chutimanitsakun, A. Corey, T. Filichkina, N. García-Mariño, I. Romagosa, and P. M. Hayes (2011). Comparative mapping of the oregon Wolfe barley using doubled haploid lines derived from female and male gametes. *Theoretical and applied genetics* 122(7), 1399–1410.
- Cuthill, E. and J. McKee (1969). Reducing the bandwidth of sparse symmetric matrices. In *Proceedings of the 1969 24th national conference*, pp. 157–172. ACM.
- Felcher, K. J., J. J. Coombs, A. N. Massa, C. N. Hansey, J. P. Hamilton, R. E. Veilleux, C. R. Buell, and D. S. Douches (2012). Integration of two diploid potato linkage maps with the potato genome sequence. *PLoS One* 7(4), e36347.
- Friedman, J., T. Hastie, and R. Tibshirani (2008). Sparse inverse covariance estimation with the graphical lasso. *Biostatistics* 9(3), 432–441.
- Grandke, F., S. Ranganathan, N. van Bers, J. R. de Haan, and D. Metzler (2017). Pergola: fast and deterministic linkage mapping of polyploids. *BMC Bioinformatics* 18(1), 12.
- Hoff, P. D. (2007). Extending the rank likelihood for semiparametric copula estimation. *The Annals of Applied Statistics*, 265–283.
- Jansen, J., A. De Jong, and J. Van Ooijen (2001). Constructing dense genetic linkage maps. *Theoretical and Applied Genetics* 102(6-7), 1113–1122.
- Liu, H., F. Han, M. Yuan, J. Lafferty, and L. Wasserman (2012). High-dimensional semiparametric gaussian copula graphical models. *The Annals of Statistics*, 2293–2326.
- Margarido, G., A. Souza, and A. Garcia (2007). Onemap: software for genetic mapping in outcrossing species. *Hereditas* 144(3), 78–79.
- Massa, A. N., N. C. Manrique-Carpintero, J. J. Coombs, D. G. Zarka, A. E. Boone, W. W. Kirk, C. A. Hackett, G. J. Bryan, and D. S. Douches (2015). Genetic linkage mapping of economically important traits in cultivated tetraploid potato (*solanum tuberosum* l.). *G3: Genes—Genomes—Genetics* 5(11), 2357–2364.

- McLachlan, G. and T. Krishnan (2007). *The EM algorithm and extensions*, Volume 382. John Wiley & Sons.
- Preedy, K. and C. Hackett (2016). A rapid marker ordering approach for high-density genetic linkage maps in experimental autotetraploid populations using multidimensional scaling. *Theoretical and Applied Genetics* 129(11), 2117–2132.
- Stam, P. (1993). Construction of integrated genetic linkage maps by means of a new computer package: Join map. *The Plant Journal* 3(5), 739–744.
- Voorrips, R. E. and C. A. Maliepaard (2012). The simulation of meiosis in diploid and tetraploid organisms using various genetic models. *BMC bioinformatics* 13(1), 248.
- Wang, H., F. A. van Eeuwijk, and J. Jansen (2016). The potential of probabilistic graphical models in linkage map construction. *Theoretical and Applied Genetics*, 1–12.
- Wu, Y., P. R. Bhat, T. J. Close, and S. Lonardi (2008). Efficient and accurate construction of genetic linkage maps from the minimum spanning tree of a graph.
- Yin, J. and H. Li (2011). A sparse conditional gaussian graphical model for analysis of genetical genomics data. *The annals of applied statistics* 5(4), 2630.